Research Article

NEURAL REGENERATION RESEARCH
www.nrronline.org

Magnesium-L-threonate treats Alzheimer's disease by modulating the microbiota-gut-brain axis

Wang Liao[1, #], Jiana Wei[1, 2, #], Chongxu Liu[1, #], Haoyu Luo[1], Yuting Ruan[3], Yingren Mai[1], Qun Yu[4], Zhiyu Cao[4], Jiaxin Xu[4], Dong Zheng[5], Zonghai Sheng[6], Xianju Zhou[2, *], Jun Liu[1, *]

https://doi.org/10.4103/1673-5374.391310

Date of submission: June 30, 2023

Date of decision: October 7, 2023

Date of acceptance: November 6, 2023

Date of web publication: December 21, 2023

From the Contents

Graphical Abstract

Magnesium-L-threonate improves cognition, alleviates oxidative stress and inflammation in APP/PS1 mice by modulating the microbiota-gut-brain axis

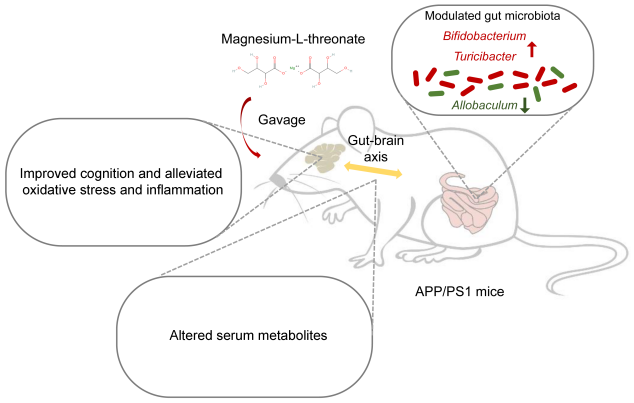

Abstract

Disturbances in the microbiota-gut-brain axis may contribute to the development of Alzheimer's disease. Magnesium-L-threonate has recently been found to have protective effects on learning and memory in aged and Alzheimer's disease model mice. However, the effects of magnesium-L-threonate on the gut microbiota in Alzheimer's disease remain unknown. Previously, we reported that magnesium-L-threonate treatment improved cognition and reduced oxidative stress and inflammation in a double-transgenic line of Alzheimer's disease model mice expressing the amyloid-β precursor protein and mutant human presenilin 1 (APP/PS1). Here, we performed 16S rRNA amplicon sequencing and liquid chromatography-mass spectrometry to analyze changes in the microbiome and serum metabolome following magnesium-L-threonate exposure in a similar mouse model. Magnesium-L-threonate modulated the abundance of three genera in the gut microbiota, decreasing *Allobaculum* and increasing *Bifidobacterium* and *Turicibacter*. We also found that differential metabolites in the magnesium-L-threonate-regulated serum were enriched in various pathways associated with neurodegenerative diseases. The western blotting detection on intestinal tight junction proteins (zona occludens 1, occludin, and claudin-5) showed that magnesium-L-threonate repaired the intestinal barrier dysfunction of APP/PS1 mice. These findings suggest that magnesium-L-threonate may reduce the clinical manifestations of Alzheimer's disease through the microbiota-gut-brain axis in model mice, providing an experimental basis for the clinical treatment of Alzheimer's disease.

Key Words: Alzheimer's disease; APP/PS1 double-transgenic Alzheimer's disease mouse model; inflammation; intestinal barrier dysfunction; magnesium-L-threonate; microbiome; microbiota-gut-brain axis; oxidative stress; serum metabolites

Introduction

Alzheimer's disease (AD) is one of the most serious age-related diseases and, along with cardiovascular diseases and tumors, is a leading cause of death (Tiwari et al., 2019). As one of the most complex, multifactorial, and mechanism-mediated diseases, AD involves multiple genes and targets, and can be triggered by various factors (Holtzman et al., 2011). The human body hosts many bacteria and other microorganisms that are collectively referred to as the microbiota; these microbes and their respective genomes comprise the microbiome. The human microbiome plays an important role in regulating the health of certain bodily systems, such as the

[1]Department of Neurology, The Second Affiliated Hospital of Guangzhou Medical University, Guangzhou, Guangdong Province, China; [2]Special Medical Service Center, Neuroscience Center, Integrated Hospital of Traditional Chinese Medicine, Southern Medical University, Guangdong, Guangdong Province, China; [3]Department of Rehabilitation, The Second Affiliated Hospital, Guangzhou Medical University, Guangzhou, Guangdong Province, China; [4]Department of Neurology, Sun Yat-sen Memorial Hospital, Sun Yat-sen University, Guangzhou, Guangdong Province, China; [5]Department of Neurology, The Affiliated Brain Hospital of Guangzhou Medical University, Guangzhou, Guangdong Province, China; [6]Institute of Biomedical and Health Engineering, Shenzhen Institute of Advanced Technology, Chinese Academy of Sciences, Shenzhen, Guangdong Province, China

***Correspondence to:** Xianju Zhou, PhD, xianjuzhou2022@163.com; Jun Liu, PhD, liujun@gzhmu.edu.cn.

https://orcid.org/0000-0003-0526-3523 (Jun Liu); https://orcid.org/0000-0003-1744-556X (Xianju Zhou)

#These authors contributed equally to this paper.

Funding: *This study was supported by the National Natural Science Foundation of China, Nos. 82101271 (to WL), 82171178 (to JL); Basic and Applied Basic Research Foundation of Guangdong Province, Nos. 2020A1515110317 (to WL), 2021A1515010705 (to WL); Young Talent Support Project of Guangzhou Association for Science and Technology (to WL) and Technology Key Project of Shenzhen, No. JCYJ20200109114612308 (to ZS).*

How to cite this article: *Liao W, Wei J, Liu C, Luo H, Ruan Y, Mai Y, Yu Q, Cao Z, Xu J, Zheng D, Sheng Z, Zhou X, Liu J (2024) Magnesium-L-threonate treats Alzheimer's disease by modulating the microbiota-gut-brain axis. Neural Regen Res 19(10):2281-2289.*

immune system (Wu and Wu, 2012). The microbiome-gut-brain axis refers to the functional response of gut microbes to the gut-brain axis in humans (Liu et al., 2022; Claudino Dos Santos et al., 2023). Microorganisms influence neural pathways by regulating the circulation of immune factors and metabolites, which, in turn, affect neurodegenerative diseases. The microbiome-gut-brain axis plays a crucial role in communicating information from the gut to the brain (Carabotti et al., 2015). Internal and external changes, particularly those caused by the long-term use of broad-spectrum antibiotics, inhibit the growth of sensitive intestinal bacteria, allowing uninhibited bacteria to multiply and resulting in dysbiosis. In this situation, the normal physiological balance of bacteria is disrupted, enabling entry of pathogens and accumulation of toxic metabolites. Evidence that intestinal dysbiosis plays a role in the pathogenesis of diseases of the central nervous system (CNS) is increasing (Alsegiani and Shah, 2022; Chidambaram et al., 2022b). A clinical study confirmed that gastrointestinal symptoms often appear within the first few years of the development of neurodegenerative diseases (Katsuno et al., 2018). Pathogens and toxic metabolites enter the systemic circulation, leading to the dysregulation of glucocerebrosidase and chronic neuroinflammation through dysregulation of immune activation, triggering the release of neurotoxic, misfolded proteins into the systemic circulation (Kaur et al., 2021). Accumulation of these proteins in and around CNS cells leads to neuronal death. A direct correlation was identified between dysregulation of the intestinal flora and exacerbation and spread of neurodegenerative diseases (Chidambaram et al., 2022a).

Intestinal bacteria can affect brain function, causing neurodegenerative disorders and influencing the interaction between the immune and nervous systems, altering immune system regulation (Fung et al., 2017; Ichikawa et al., 2023). The lipopolysaccharides found in amyloid plaques and the blood vessels surrounding them in the brains of patients with AD are also pro-inflammatory compounds. The gut microbiota produces metabolites with anti-inflammatory and neuroprotective effects on the brain (Marizzoni et al., 2020). A 2017 study reported distinct differences in gut microbial composition between patients with AD and healthy people, and the levels of several of those bacteria in the gut and cerebrospinal fluid were positively correlated with concentrations of AD-related biomarkers (Mothapo et al., 2017). These patients exhibited reduced gut microbial diversity, with overrepresention of some bacteria and greatly reduced abundance of others (Marizzoni et al., 2020; Trejo-Castro et al., 2022).

Magnesium is the fourth most abundant cation in the human body regulating the electron flow of various ion channels and catalyzing many biological and chemical reactions (Jahnen-Dechent and Ketteler, 2012). Magnesium regulates central neurotransmitters, such as catecholamines, opioid receptors, and neuroDNA receptors, by inhibiting sodium-potassium-ATPase and magnesium-ATPase, thereby affecting CNS function and regulating nerve function via hormones (Abumaria et al., 2011). In our previous study, magnesium-L-threonate (MgT), considered a dietary food supplement, demonstrated significant neuroprotective effects against oxidative stress in a double-transgenic line of AD model mice expressing the amyloid-β precursor protein and mutant human presenilin 1 (APP/PS1) (Xiong et al., 2022).

Because the gut microbiota and magnesium each play roles in modulating AD, we hypothesized that MgT intake might interact with the gut microbiota to alleviate AD. Although the effect of MgT on the gut microbiota has not been investigated, a study found that dietary magnesium supplementation affects the abundance of intestinal flora (Piuri et al., 2021). Here, we aimed to determine whether MgT ameliorates AD by modulating the microbiota-gut-brain axis, focusing on its effects on the gut microbiota using the APP/PS1 mouse model. Hematoxylin and eosin (H&E) staining of colon tissues was used to identify inflammatory factors and oxidative stress indices in MgT-treated APP/PS1 mice. We also used 16S rRNA amplicon sequencing and liquid chromatography-mass spectrometry (LC-MS) to analyze changes in the microbiome and serum metabolome of these mice.

Methods

Mice

Six-month-old male APP/PS1 transgenic mice (stock No. 110322220100981143; RRID: MMRRC_034829-JAX), weighing 20–25 g, and age- and sex-matched wild-type C57BL/6J mice (stock No. 110324220102277936; RRID: IMSR_JAX:000664), weighting 20–25 g, were obtained from Beijing Vital River Laboratory Animal Technology Co., Ltd. (Beijing, China; Certification No. SCXK (Jing) 2019-0009). Male mice were used in reference to the previously published protocol (Xiong et al., 2022; Zhang et al., 2023). During the dark period of 12 hours, the mice were allowed to freely consume food and water in a separate, ventilated cage with a temperature of 22–25°C and relative humidity of 50–60%. All procedures and experiments were approved by the Institutional Animal Care and Use Committee of Sun Yat-Sen University (approval No. SYSU-IACUC-2020-B1017) on August 25, 2020. All experiments were designed and reported in accordance with the Animal Research: Reporting of *In Vivo* Experiments (ARRIVE) guidelines (Percie du Sert et al., 2020).

Drug administration

The mice were assigned to three groups (n = 5 per group): wild-type C57BL/6J mice (WT), APP/PS1 mice (APP/PS1), and APP/PS1 mice treated with MgT (MgT). MgT (M843873; Guangzhou Yongjin Biotechnology Co., Ltd., Guangzhou, Guangdong, China) was administered to the MgT group at 910 mg/kg daily via drinking water, as described in our previous study (Xiong et al., 2022). The other two groups received regular drinking water only. After 1 month with or without MgT treatment, the mice were subjected to the Morris water maze test, then sacrificed under deep anesthesia with intraperitoneal injection of 150 mg/kg pentobarbital sodium (Sanci Biotechnology Co., Ltd., Shanghai, China) to collect colon tissues, feces, and serum for further analysis (**Figure 1**).

Morris water maze test

Morris water maze tests were conducted to monitor spatial

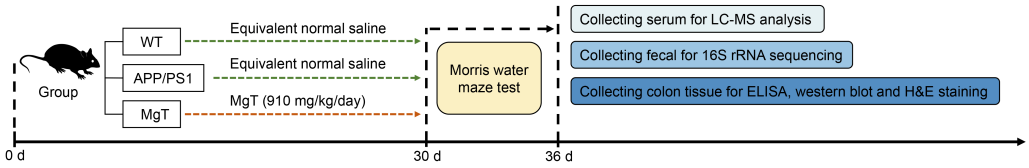

Figure 1 | **Experimental flow chart.**
APP/PS1: Amyloid-β precursor protein and mutant human presenilin 1; ELISA: enzyme-linked immunosorbent assay; H&E: hematoxylin and eosin; LC-MS: liquid chromatography-mass spectrometry; MGT: magnesium-L-threonate; WT: wild-type.

memory and learning (Liu et al., 2019). A round container (Yiyunrui Biotechnology Co., Ltd., Guangzhou, Guangdong, China) with a radius of 60 cm and a height of 50 cm was divided into four quadrants for use in the test. A concealed escape platform with a 4.5-cm radius was placed 2 cm underwater, at the center of the divided quadrant. Water for the WT and APP/PS1 mice was stained with titanium dioxide and adjusted to 22°C. Several visual cues were provided by the container, which was placed in a poorly lit, soundproof room. Five consecutive days were dedicated to conducting the directional navigation tests. Various starting positions were selected for the mice to be released into the pool of water, and they were allowed to swim until they reached the hidden platform. This test was repeated four times a day at 30-minute intervals. The delay time to reach the platform and swimming trajectory (maximum duration: 90 seconds) were measured using a computer-controlled video tracking system developed by the Institute of Medicine of the Chinese Academy of Medical Sciences (Beijing, China). When the mice were placed on the hidden platform directly, a 15-second period was allowed to pass before they reached it. The escape latency was determined by the time taken to reach the platform from the starting point. On the 6th day, the platform was removed from the site. The mice were released opposite to the platform and allowed to swim through the maze for 90 seconds.

Assessment of oxidative stress levels and inflammation in colon tissue

Colon tissue samples were homogenized in 1 mL cold 1× phosphate-buffered saline (PBS) after flushing the excess blood with cold 1× PBS. After preparing the homogenate, it was centrifuged at 5000 × *g* for 5 minutes. The supernatant was evaluated as follows: enzyme-linked immunosorbent assay (ELISA) kits (Jiangsu Meimian Industrial Co., Ltd., Nanjing, Jiangsu, China) were used to detect the pro-inflammatory cytokines tumor necrosis factor (TNF)-α and interleukin (IL)-1β, and the anti-inflammatory cytokine IL-10; and spectrophotometric kits (Jiangsu Meimian Industrial Co., Ltd.) were used to detect oxidative indices malondialdehyde (MDA), catalase (CAT), and superoxide dismutase (SOD). All tests were conducted in accordance with the respective manufacturer's guidelines. Detection of ELISA and spectrophotometry results were conducted on a Thermo Labsystems Multiskan MS 352 microplate reader (Ascent, Finland) and an automatic biochemical analyzer (AU480; Beckman Coulter Ltd., Pasadena, CA, USA), respectively.

Fecal DNA extraction and 16S rRNA sequencing

The V3–V4 hypervariable region of the bacterial 16S ribosomal DNA (rDNA) was amplified using 20–30 ng DNA. Paired primers were designed by Magigene Ltd. (Shenzhen, China). The forward and reverse primers for 16S rDNA amplification were 5′-ACT CCT ACG GGA GGC AGC A-3′ and 5′-GGA CTA CHV GGG TWT CTA AT-3′, respectively. Polymerase chain reaction (PCR) amplification was performed in triplicate and each reaction volume contained 2.5 μL TransStart Buffer (TransGen, Beijing, China), 2.5 μL TransStart Taq DNA polymerase (including 2 μL dNTPs), 1 μL of each primer (100 μM), and 20–30 ng template DNA. Index adapters were connected to the ends of the amplicons to generate the indexed libraries. Quality control of the PCR products with index adapters was performed using a Qubit 3.0 Fluorometer (Invitrogen, Carlsbad, CA, USA) and quantified to 10 nmol for subsequent next-generation sequencing. The DNA libraries were loaded onto an Illumina MiSeq platform (San Diego, CA, USA) in accordance with the manufacturer's instructions, and sequencing was performed using the paired-end 250-base pair mode.

FastP software (version 0.18.0) was used to trim the raw reads to generate clean reads (Chen et al., 2018). The clean reads were assembled into raw tags using FLASH software (version 1.2.11) (Magoč and Salzberg, 2011). After chimera filtration, the effective tags were clustered into operational taxonomic units (OTUs) according to similarity (Edgar, 2010) using USEARCH software (version 9.2.64). A confidence threshold of 0.7 was applied to sequence classifications based on the RDP OTU Classifier version 2.2 of the 16S rRNA database (Silva v138) (Pruesse et al., 2007; Wang et al., 2007).

Microbial community analysis

For microbial community analysis, we excluded OTUs with < 0.005% sequence reads. The α-diversity index was calculated in QIIME (Caporaso et al., 2010), and comparisons of this index between groups was computed by Tukey's honestly significant difference test in the R project vegan package (version 2.5.3) (Oksanen et al., 2022). Principal coordinates analysis (PCoA) of Bray–Curtis distances was generated in the R project vegan package and plotted in the R project ggplot2 package (version 2.2.1) (Wickham, 2016). Statistical analysis of the analysis of similarities (ANOSIM) test was performed using the R project vegan package. A stacked bar plot of the community composition was visualized using the R project ggplot2 package. Linear discriminant analysis of effect size (LEfSe) was used to characterize the biomarker features in each group with the following cutoffs: linear discriminant analysis (LDA) scores (log10) > 3 and P values < 0.05. The Kyoto Encyclopedia of Genes and Genomes (KEGG) pathway analysis of the OTUs was performed using Tax4Fun (version 1.0) (Aßhauer et al., 2015). Functional differences between groups were analyzed using Welch's t-test in the R project vegan package.

Serum metabolite extraction and LC-MS analysis

The serum samples were thawed and vibrated for 10 seconds; 50 µL of each vortexed sample was transferred to a centrifuge tube; 300 µL 20% acetonitrile-methanol internal standard extract was added to each sample, followed by vortexing for 3 minutes and centrifuging at 14,000 × *g* for 10 minutes at 4°C. After centrifugation, 200 µL of supernatant was pipetted into a new centrifuge tube, stored at –20°C for 30 minutes, then spun again at 12,000 r/min for 3 minutes at 4°C; 180 µL supernatant was transferred into the sample bottle and used for chromatographic analysis. Metabolome analysis was performed by Magigene Ltd. using an Agilent UHPLC 1290 Infinity-Triple Quad MS 6460 equipped with an electrospray ionization source (Agilent Technologies Inc., Santa Clara, CA, USA). Using 0.1% formic acid aqueous solution as the mobile phase (A) and acetonitrile as the stationary phase (B), the metabolites in the sample bottle were determined using a Zorbax SB-C18 column (Agilent Technologies Inc.). A gradient elution of 5% (v/v) B occurred between 0 and 0.5 minutes, 10% B between 0.5 and 2 minutes, 40% B between 2 and 5 minutes, and 90% B between 2 and 5 minutes. The column had a flow rate of 0.3 mL/min at a temperature of 40°C. The MS parameters were as follows: capillary voltage, 4.0 kV; nozzle voltage, 500 V; 45 psi sprayer; gas temperature, 300°C; sheath temperature, 350°C; gas flow, 13 L/min. The raw data were converted to the mzML format using ProteoWizard software, and the XCMS program was used for peak extraction, alignment, and retention time correction of the mzML files. The support vector regression method was used to correct the peak area and to filter peaks with > 50% missing data in each sample group. Metabolite identification information was obtained by searching the laboratory's own database and integrating public and artificial intelligence prediction libraries.

Partial least squares discriminant analysis (PLS-DA) was applied to group comparisons using the R package models to identify metabolite abundance. The variable importance in projection (VIP) score of the partial least squares model was used to rank the metabolites that best distinguished the two groups and *t*-tests for univariate analysis were used to screen for differential metabolites between the two groups, with the following cutoffs: VIP scores ≥ 1 and *t*-test *P* values < 0.05. The KEGG pathway enrichment of differential metabolites was performed using a hypergeometric test with a threshold of $P < 0.05$.

Microbiome and metabolome interaction analyses

Relationships between the differential microbes (genus level), differential metabolites, and pro-inflammatory and anti-inflammatory cytokine indices were estimated using Spearman's correlation coefficient. Connection retention was saved while satisfying the thresholds of absolute correlation values > 0.5 and *P* values < 0.05. Interaction networks were visualized using Cytoscape v3.8.2 (Chen et al., 2009).

H&E staining of colon tissues

Alcohol was used to dehydrate the tissues after removal from the 10% buffered formalin. Paraffin wax-embedded, dehydrated tissue sections were stained with H&E (G1003; Servicebio, Wuhan, China) in accordance with the manufacturer's recommendations. The Leica Application Suite v4 (Wetzlar, Germany) was used to examine the stained cells. Using Image-Pro Plus 6.1 software (Media Cybernetics, Inc., Rockville, MD, USA), we estimated the fat percentage and jejunal villus height.

Assessment of intestinal barrier dysfunction

To assess intestinal barrier dysfunction, we measured the levels of three intestinal tight junction proteins: zona occludens 1 (ZO-1), occludin, and claudin-5. For western blotting, colon tissues were lysed in freshly prepared radioimmunoprecipitation assay buffer (50 mM Tris-buffered saline, 0.5% deoxysodium cholate, 1 mM ethylene diamine tetraacetic acid, 150 mM NaCl, 1% NP-40, and 1 mM phenylmethylsulfonyl fluoride). The concentrations of the protein extracts were determined using a bicinchoninic acid protein assay kit (Solarbio, Beijing, China). Proteins (50 µg per lane) were separated by sodium dodecyl sulfate-polyacrylamide gel electrophoresis and transferred onto polyvinylidene difluoride membranes (Merck Millipore Co., Ltd., Darmstadt, Baden-Württemberg, Germany). The membranes were blocked with 5% bovine serum albumin prepared in pH 7.5 Tris-buffered saline containing 0.1% Tween-20 for 1 hour at room temperature, then incubated with the primary antibodies overnight at 4°C, followed by the horseradish peroxidase-conjugated secondary goat antibodies (1:5000, Cat# S0002, RRID: AB_2839430; Affinity Biosciences Ltd., Changzhou, Jiangsu, China). The primary rabbit antibodies (all from Affinity Biosciences Ltd.) were as follows: ZO-1 (1:500, Cat# AF5145, RRID: AB_2837631), occludin (1:3000, Cat# DF7504, RRID: AB_2841004), claudin-5 (1:3000, Cat# AF5216, RRID: AB_2837702), and β-actin (1:5000, Cat# AF7018, RRID: AB_2839420). Protein bands were visualized using a femto-sensitive enhanced chemiluminescent solution (Mikx Biotechnology Co., Ltd., Shanghai, China) on an iBright gel imaging system (Invitrogen).

Statistical analysis

Data were analyzed using SPSS software (version 17.0; SPSS Corporation, Chicago, IL, USA). Data are presented as means and standard errors of the mean (SEMs). One-way analysis of variance followed by Tukey's honestly significant difference test was used to compare multiple groups. Significance was set at $P < 0.05$.

Results

MgT improves cognition and alleviates colonic oxidative stress and inflammation in APP/PS1 mice

Behavioral performance was examined using the Morris water maze method. As expected based on our previous study, the cognitive deficits exhibited by APP/PS1 mice were ameliorated by treatment with MgT (**Figure 2A**). Administration of MgT also significantly restored the memory function of APP/PS1 mice to the levels observed in WT mice (**Figure 2B**). Oxidative and inflammatory parameters were also assessed. Serum MDA levels significantly decreased (**Figure 2C**), whereas the levels of the antioxidant factors SOD and CAT significantly increased (**Figure 2D** and **E**), following MgT supplementation.

Furthermore, the MgT-treated group exhibited significantly lower levels of pro-inflammatory cytokines, including TNF-α and IL-1β (**Figure 2F** and **G**), and increased levels of the anti-inflammatory cytokine IL-10 (**Figure 2H**).

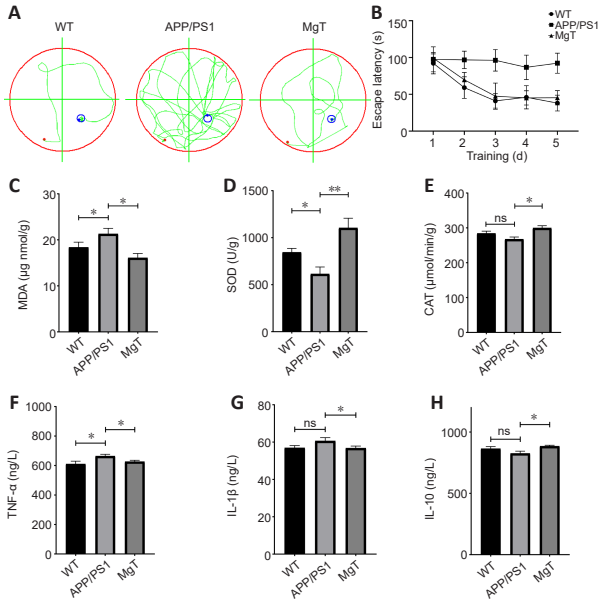

Figure 2 | Protective effects of MgT against oxidative stress and inflammation-related damage to the colons of APP/PS1 mice.
(A) Diagram of the Morris water maze and the swimming trajectories (green lines) of mice in each group. Blue circles represent the platform, and red dots indicate the point at which the mice set off. (B) Escape latency time for each group. (C–H) Levels of MDA (C), SOD (D), CAT (E), and pro-inflammatory cytokines TNF-α (F), IL-1β (G), and IL-10 (H) in each group. The results are presented as means ± SEM (n = 5), analyzed by one-way analysis of variance followed by Tukey's honestly significant difference test; *P < 0.05 and **P < 0.01. APP/PS1: Amyloid-β precursor protein and mutant human presenilin 1; CAT: catalase; IL: interleukin; MDA: malondialdehyde; MGT: magnesium-L-threonate; SOD: superoxide dismutase; TNF: tumor necrosis factor; WT: wild-type.

MgT modulates the gut microbiota of APP/PS1 mice

The gut microbiota structure of the three groups was analyzed using 16S rDNA high-throughput sequencing. A total of 1216 OTUs obtained using high-throughput sequencing were annotated. According to the α-diversity analysis, MgT significantly increased the Shannon and Simpson indices in APP/PS1 mice (**Figure 3A**). PCoA of β-diversity showed that the three groups were separately clustered (**Figure 3B**). The ANOSIM test of β-diversity indicated a significant difference in bacterial diversity among the three groups (R = 0.86, P = 0.001; **Figure 3C**). Compared with the APP/PS1 group, at the phylum level, the MgT group had decreased abundances of *Proteobacteria* and *Firmicutes* and increased abundance of *Bacteroidetes* (**Figure 3D**); at the genus level, the MgT group had decreased abundances of *Allobaculum* and *Desulfovibrio* and increased abundance of *Bifidobacterium* (**Figure 3E**).

Next, we used LEfSe analysis to estimate the biomarkers correlated with MgT treatment. Compared with the APP/PS1 group, the MgT group had increased abundances of *Breve*, *Pseudolongum*, *Actinobacteria*, *Bifidobacteriales*, and *Bifidobacteriaceae*. Simultaneously, the abundances of *Allobaculum*, *Erysipelptrichaceae*, and other flora decreased in the MgT group compared to those in the APP/PS1 group (**Figure 4A**). Differences in the functional flora pathways between the MgT and APP/PS1 groups were mainly reflected by differences in oxidative phosphorylation function, D-alanine metabolism function, and ATP-binding cassette transporter function-related pathways. Among these, the ABC transporter function-related differences were the most obvious, suggesting that the regulation of transporter expression may be related to the therapeutic mechanism of MgT (**Figure 4B**).

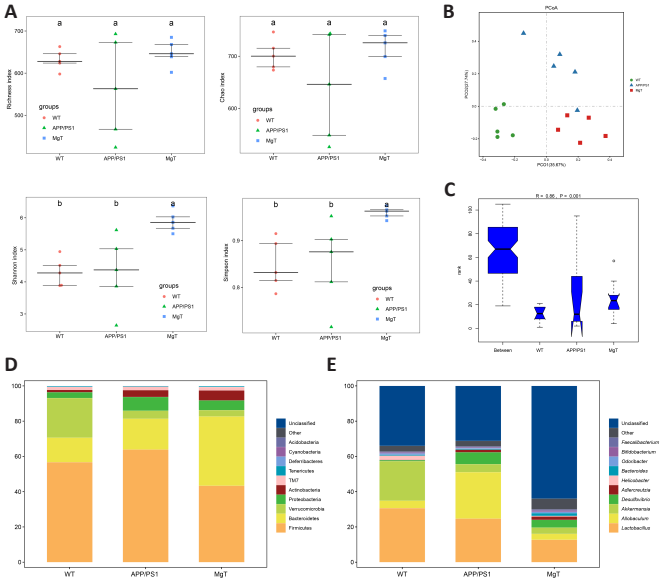

Figure 3 | Group comparisons of microbial diversity and community composition.
(A) α-Diversity of the gut microbiota in the three groups, as measured by Richness, Chao, Simpson, and Shannon indices. Lowercase letters a and b indicate significant differences (P < 0.05), as determined by one-way analysis of variance and Tukey's least significant difference test. (B) PCoA plot of β-diversity metrics based on the Bray-Curtis distance matrix of the relative abundances of bacterial taxa. Each point in the PCoA plot represents one sample, and samples from the different groups are shown in different colors. (C) Comparison of β-diversity differences between the sample groups using an ANOSIM test. (D, E) Microbial composition of the three groups at the phylum level (D) and the genus level (E). MGT: Magnesium-L-threonate; PcoA: principal coordinates analysis; WT: wild-type.

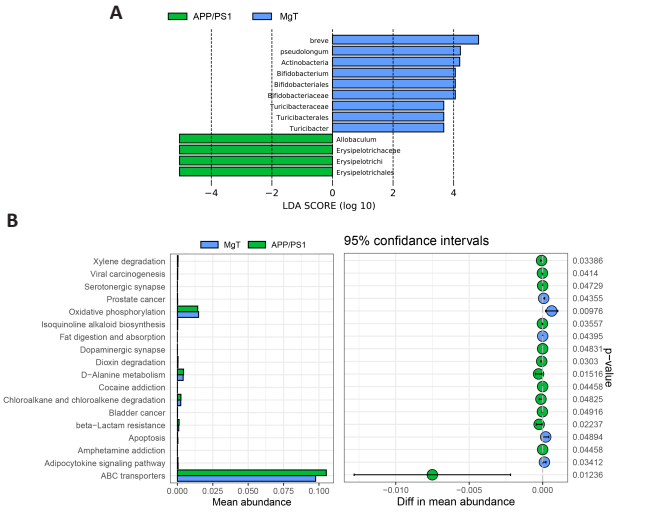

Figure 4 | Differences in gut microbiota and abundance of related functional pathways between MgT and APP/PS group mice.
(A) LDA scores of LEfSe (cutoffs: log10 > 3 and P < 0.05) of fecal bacteria, revealing significant differences between the MgT and APP/PS1 groups. (B) Functional pathways of the gut microbiota with differential abundance between the MgT and APP/PS1 groups, as determined by Welch's t-test. APP/PS1: Amyloid-β precursor protein and mutant human presenilin 1; LDA: linear discriminant analysis; MGT: magnesium-L-threonate.

MgT changes the serum metabolites in APP/PS1 mice

We detected 930 metabolites in the serum metabolome of all groups (**Additional Table 1**). PLS-DA plots illustrated the differences in mouse serum metabolites among the three groups (**Figure 5A** and **B**). Comparisons of differential metabolites among the three groups showed that the MgT versus WT comparison had the lowest number of differential metabolites, with eight upregulated metabolites and one downregulated metabolite (**Figure 5C**). Differential metabolite heat maps of the APP/PS1 versus WT and MgT groups are shown in **Figure 6A** and **B**. The KEGG pathways of differential metabolites with enrichment in the MgT group compared with that in the APP/PS1 group were mainly related to metabolism, but were also related to key pathways associated with neurodegenerative diseases, including sphingolipid signaling, Parkinson's disease, neuroactive ligand-receptor interaction, and others (**Figure 6C**).

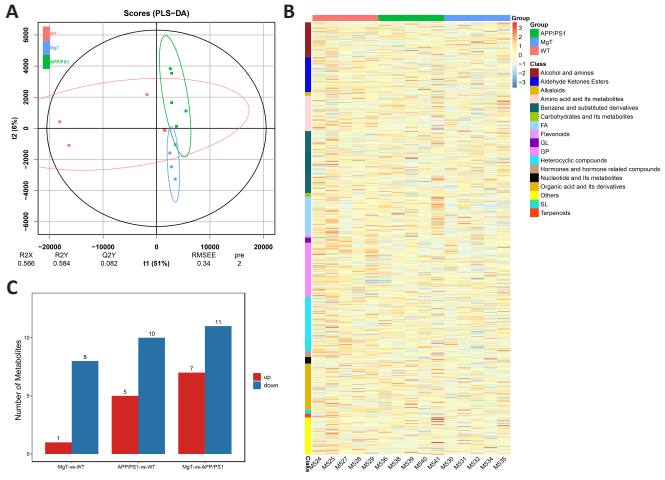

Figure 5 | Identification of serum metabolites significantly altered by MgT treatment in APP/PS1 mice.

(A) PLS-DA plot of serum metabolites in the three groups of mice. (B) Heatmap of relative abundance of all detected metabolites in all samples of the three groups. (C) Numbers of differentially upregulated and downregulated metabolites in each group comparison. APP/PS1: Amyloid-β precursor protein and mutant human presenilin 1; MGT: magnesium-L-threonate; PLS-DA: partial least squares discriminant analysis.

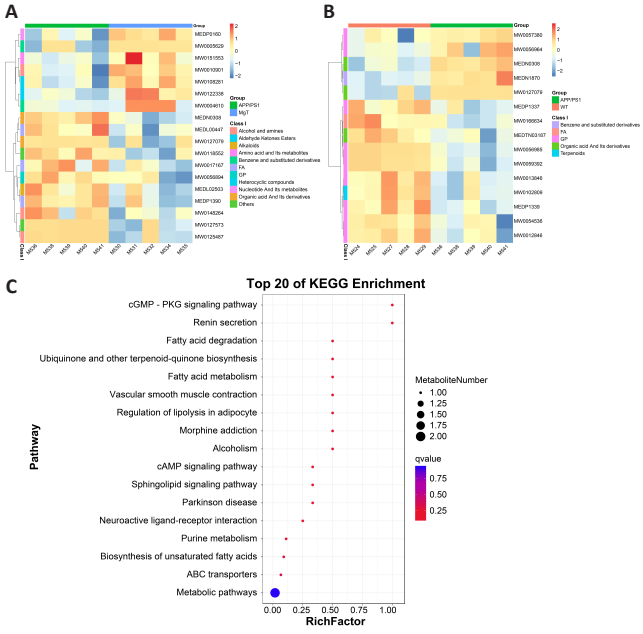

Figure 6 | Functional analysis of the differential metabolites between the three groups of mice.

Heatmap illustrating the differential metabolites between the APP/PS1 and WT groups (A) and the APP/PS1 and MgT groups (B). (C) KEGG pathway enrichment analysis of the differential metabolites between the MgT and APP/PS1 groups. APP/PS1: Amyloid-β precursor protein and mutant human presenilin 1; KEGG: kyoto Encyclopedia of Genes and Genomes; MGT: magnesium-L-threonate; WT: wild-type.

Correlations between MgT-regulated bacteria and metabolites in mice

Comparison of the intestinal microbiota between the MgT and APP/PS1 groups mainly revealed differences in the abundances of Allobaculum, Bifidobacterium, and Turicibacter. These bacteria were associated with oxidative stress and the levels of inflammatory factors, including MDA, SOD, CAT, TNF-α, IL-1, and IL-10 (**Figure 7A**). The differential serum metabolites between the MgT and APP/PS1 groups are shown in **Figure 7B**, revealing metabolites associated with neurodegenerative diseases (**Figure 7B** and **C**). These findings indicated that MgT regulates the release of gut inflammatory factors by regulating the abundance of certain intestinal bacteria. Inflammatory factors were found to further regulate the content of serum metabolites and affect neurodegenerative-related pathways in the brain, thereby alleviating the severity of AD in model mice (**Figure 7D**).

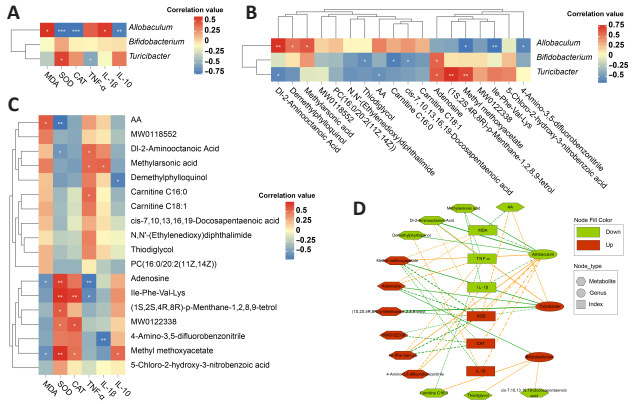

Figure 7 | Relationships between altered gut bacteria and metabolites regulated by MgT in APP/PS1 mice.

(A, B) Correlations between the abundance of three bacterial genera and oxidative stress and inflammation indices (A) and metabolites (B) with differences between the MgT and APP/PS1 groups. (C) Correlations between oxidative stress and inflammation indices and the abundance of these differential metabolites. Significant correlations between each pairwise index are expressed as $*P < 0.05$, $**P < 0.01$, and $***P < 0.001$. (D) Interaction network illustrating the role of these important bacterial genera and differential metabolites in the regulation of oxidative stress and inflammatory responses. APP/PS1: Amyloid-β precursor protein and mutant human presenilin 1; CAT: catalase; IL: interleukin; MDA: malondialdehyde; MGT: magnesium-L-threonate; SOD: superoxide dismutase; TNF: tumor necrosis factor.

MgT protects against the intestinal pathology and barrier dysfunction of APP/PS1 mice

To investigate the effects of MgT on the intestinal pathology of APP/PS1 mice, we examined histopathological changes in the colon. H&E staining confirmed that the colonic mucosal epithelium of the WT group was intact, the intestinal glands were abundant and tightly arranged, goblet cells were abundant, and there were no evident abnormalities in cell

morphology. In the APP/PS1 group, H&E staining revealed slight mucosal epithelial cell damage, hyperchromatic nuclear pyknosis, enhanced eosinophilia in the cytoplasm, and occasional slight inflammatory cell infiltration into the lamina propria. By contrast, in the MgT treatment group, the mucosal epithelium was intact, the intestinal glands were abundant and tightly arranged, goblet cells were abundant, and cell morphology was normal with no evident abnormalities (**Figure 8A**).

The levels of tight junction proteins were also determined to further examine the effects of MgT treatment on intestinal integrity. The colonic levels of ZO-1, occludin, and claudin-5 were significantly lower in APP/PS1 mice than in WT mice, but were significantly restored by MgT treatment (**Figure 8B**).

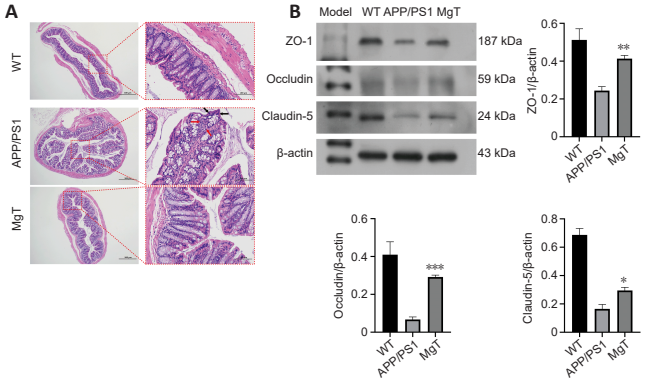

Figure 8 | MgT-mediated protection against intestinal pathology and barrier dysfunction of APP/PS1 mice.

(A) Hematoxylin and eosin staining of representative colonic tissues from the three groups. Compared with the WT and MgT groups, the APP/PS1 group showed slight mucosal epithelial cell damage, hyperchromatic nuclear pyknosis, enhanced eosinophilia in the cytoplasm (black arrows), and slight inflammatory cell infiltration in the lamina propria (red arrows). (B) Western blotting and quantification of protein levels of ZO-1, occludin, and claudin-5 in the WT, APP/PS1, and MgT groups. Results presented as means ± SEM (n = 3), analyzed by one-way analysis of variance followed by Tukey's honestly significant difference test; *P < 0.05, **P < 0.01, and ***P < 0.001 between the APP/PS1 and MgT groups. APP/PS1: Amyloid-β precursor protein and mutant human presenilin 1; MGT: magnesium-L-threonate; WT: wild-type; ZO-1: zona occludens 1.

Discussion

The gut microbiota continuously interacts with the nervous, immune, and endocrine systems to ensure the proper development and function of each system (Maranduba et al., 2015; Ma et al., 2019; Ghosh and Pramanik, 2021; Pluta and Januszewski, 2023). The importance of such communication is illustrated by the microbiota-gut-brain axis, a bidirectional communication network that links the enteric system and CNS (Fernández-Tomé et al., 2021) and thus determines an individual's health status. This bidirectional axis is formed during infancy and is influenced by many environmental and lifestyle factors, such as diet and stress. It has also been shown to be essential for maintaining homeostasis, which affects health and aging (Larroya et al., 2021). Consequently, changes in the gut microbiota associated with dysbiosis, gut barrier degradation, and inflammatory conditions affect the immune, endocrine, and nervous systems, as well as all other parts of the body. Additionally, this mechanism is involved in several pathologies, including altered brain function (Hou et al., 2022). Inflammatory system aging degenerates the microbiota and homeostatic system, thereby increasing the risk of aging-related pathologies, such as neurodegenerative diseases (Rea et al., 2018). The microbiota-gut-brain axis is known to play a role in AD pathogenesis and is currently an important target for preventing and slowing AD development.

Magnesium is necessary for > 300 biochemical reactions in the body and has become a focus of brain health (Fiorentini et al., 2021). Magnesium restores nerve cell health, and recent human clinical studies have reported dramatic improvements in memory and cognition following treatment with magnesium (Wang et al., 2013). MgT occurs naturally in the body and brain and is an effective supplement for restoring magnesium levels in the brain, thereby preventing neurodegeneration and restoring brain function (Kirkland et al., 2018; Bislimi et al., 2021). MgT has also been demonstrated to have novel therapeutic effects on neurodegenerative diseases (Sahebnasagh et al., 2022). Our findings indicated that MgT treatment significantly protects the APP/PS1 mouse colon from oxidative stress and inflammatory damage. For example, MgT supplementation significantly restored the abundance of intestinal goblet cells and reduced the levels of multiple inflammatory factors. Several studies have indicated that intestinal goblet cells and inflammatory factors are associated with the abundance of certain microbial taxa in the gut (Mothapo et al., 2017; Fernández-Tomé et al., 2021; Xiong et al., 2022). In-depth studies have demonstrated that MgT improves intestinal inflammatory responses by regulating the abundance of flora in the gut, subsequently improving the inflammatory response of nerve cells through regulation of the gut-brain axis (Wang et al., 2013; Liu et al., 2021; Xiong et al., 2022). These studies elucidate the molecular mechanism for MgT-mediated neuroprotection in clinical treatment.

The intestinal bacterial genera with relatively large differences in abundance before and after MgT treatment — *Allobaculum*, *Bifidobacterium*, and *Turicibacter* — all belong to the Firmicutes phylum. Research reports on gut microbial diversity in AD have demonstrated differences in abundance rates of Bacteroidetes and Firmicutes at the phylum level between patients with AD and healthy controls (Vogt et al., 2017). Specifically, in AD patients, Bacteroidetes was more abundant and positively correlated with AD, whereas Firmicutes was less abundant and negatively correlated with AD. Interestingly, treatment with MgT significantly decreased Firmicutes and increased Bacteroidetes in APP/PS1 mice in our study. Decreased Firmicutes levels trigger inflammatory responses that are positively associated with disturbances in glycolytic metabolism (Soto-Heredero et al., 2020; Stojanov et al., 2020). Key intermediates related to glucose and lipid metabolism, such as lipids, isoleucine, lactate, alanine, glutamine, creatine, and glucose, were altered in the APP/PS1 group mice in this study, and have been closely related to patients with AD (Sato and Morishita, 2015). Furthermore, the metabolism of glucose and membrane lipids provides energy for neurons and forms a basis for cell membrane stability, respectively (Tracey et al., 2018). The MgT-treated APP/PS1 mice in this study exhibited partial restoration of glucose metabolism and lipid metabolites

to the levels observed in the WT group. Using microbiome and metabolomic strategies to identify differences in bacterial flora and metabolites between AD model and WT mice, we were able to characterize the protective mechanisms of MgT in AD, providing new insights into the pharmacodynamics of MgT in AD prevention and treatment.

Our findings also indicated the protective function of MgT against the intestinal pathology of APP/PS1 mice, which may be a common phenomenon among mice with impaired memory and learning (Bislimi et al., 2021; Fernández-Tomé et al., 2021). Downregulation of the tight junction proteins ZO-1, occludin, and claudin-5 in intestinal epithelial cells in APP/PS1 mice may cause barrier dysfunction, which may be synergistically exacerbated by the elevated inflammation in these mice. Therefore, MgT-mediated modulation of the gut microbiota appears to not only downregulate inflammation, but also recover the levels of tight junction proteins, protecting the gut-brain axis. It is possible that these results may have been biased by the use of only male mice in this study; hence, a comparison of the effects of MgT on both sexes is needed in future research.

There is a complex and close relationship between the metabolism of the gut microbiota and the CNS, and MgT-mediated regulation of the abundance of intestinal bacteria may protect the CNS (Suganya and Koo, 2020; Ojeda et al., 2021). However, the types of probiotics and prebiotics that have protective effects on the CNS signaling pathways, and the exact mechanisms that regulate nerve conduction need to be further explored. In the future, the intestinal flora may become an important target for the regulation of neurodegenerative diseases. Products that regulate the intestinal flora, such as probiotics, prebiotics, and dietary supplements such as MgT, could provide new avenues for AD treatment, but require long-term population studies. Meanwhile, whether the restored memory function of APP/PS1 mice was directly related to changes in the gut microbiota or the concentration of magnesium ions in the blood is unclear, and requires further study.

In conclusion, treatment with MgT delayed the symptoms of AD in mice by regulating the type and abundance of gut bacteria, downregulating the secretion of intestinal inflammation-related factors into the bloodstream with potentially long-term effects on the neuronal activity in the brain. These findings establish a correlation between therapeutic MgT administration and modulation of the microbiota-gut-brain axis in AD.

Author contributions: *Study design: XZ, JL; implementation of experiments: WL, JW, CL; data collection: HL, YR, YM; data analysis: QY, ZC, JX, DZ, ZS; manuscript draft: WL, JW, CL, XZ, JL. All authors have read and approved the final manuscript.*
Conflicts of interest: *The authors have no conflicts to declare.*
Data availability statement: *The datasets used and/or analysed during the current study are available in the NCBI Bioproject repository, No. PRJNA106523.*

Additional file:
Additional Table 1: *Information of metabolites identified in metabolome.*

References

Abumaria N, Yin B, Zhang L, Li XY, Chen T, Descalzi G, Zhao L, Ahn M, Luo L, Ran C, Zhuo M, Liu G (2011) Effects of elevation of brain magnesium on fear conditioning, fear extinction, and synaptic plasticity in the infralimbic prefrontal cortex and lateral amygdala. J Neurosci 31:14871-14881.

Alsegiani AS, Shah ZA (2022) The influence of gut microbiota alteration on age-related neuroinflammation and cognitive decline. Neural Regen Res 17:2407-2412.

Aßhauer KP, Wemheuer B, Daniel R, Meinicke P (2015) Tax4Fun: predicting functional profiles from metagenomic 16S rRNA data. Bioinformatics 31:2882-2884.

Bislimi K, Mazreku I, Halili J, Aliko V, Sinani K, Hoxha L (2021) Effects of vitamin C and magnesium L-threonate treatment on learning and memory in lead-poisoned mice. J Vet Res 65:217-223.

Caporaso JG, Kuczynski J, Stombaugh J, Bittinger K, Bushman FD, Costello EK, Fierer N, Peña AG, Goodrich JK, Gordon JI, Huttley GA, Kelley ST, Knights D, Koenig JE, Ley RE, Lozupone CA, McDonald D, Muegge BD, Pirrung M, Reeder J, et al. (2010) QIIME allows analysis of high-throughput community sequencing data. Nat Methods 7:335-336.

Carabotti M, Scirocco A, Maselli MA, Severi C (2015) The gut-brain axis: interactions between enteric microbiota, central and enteric nervous systems. Ann Gastroenterol 28:203-209.

Chen S, Zhou Y, Chen Y, Gu J (2018) fastp: an ultra-fast all-in-one FASTQ preprocessor. Bioinformatics 34:i884-i890.

Chen Y, Zhang R, Song Y, He J, Sun J, Bai J, An Z, Dong L, Zhan Q, Abliz Z (2009) RRLC-MS/MS-based metabonomics combined with in-depth analysis of metabolic correlation network: finding potential biomarkers for breast cancer. Analyst 134:2003-2011.

Chidambaram SB, Essa MM, Rathipriya AG, Bishir M, Ray B, Mahalakshmi AM, Tousif AH, Sakharkar MK, Kashyap RS, Friedland RP, Monaghan TM (2022a) Gut dysbiosis, defective autophagy and altered immune responses in neurodegenerative diseases: Tales of a vicious cycle. Pharmacol Ther 231:107988.

Chidambaram SB, Rathipriya AG, Mahalakshmi AM, Sharma S, Hediyal TA, Ray B, Sunanda T, Rungratanawanich W, Kashyap RS, Qoronfleh MW, Essa MM, Song BJ, Monaghan TM (2022b) The influence of gut dysbiosis in the pathogenesis and management of ischemic stroke. Cells 11:1239.

Claudino Dos Santos JC, Oliveira LF, Noleto FM, Gusmão CTP, Brito GAC, Viana GSB (2023) Gut-microbiome-brain axis: the crosstalk between the vagus nerve, alpha-synuclein and the brain in Parkinson's disease. Neural Regen Res 18:2611-2614.

Edgar RC (2010) Search and clustering orders of magnitude faster than BLAST. Bioinformatics 26:2460-2461.

Fernández-Tomé S, Ortega Moreno L, Chaparro M, Gisbert JP (2021) Gut microbiota and dietary factors as modulators of the mucus layer in inflammatory bowel disease. Int J Mol Sci 22:10224.

Fiorentini D, Cappadone C, Farruggia G, Prata C (2021) Magnesium: biochemistry, nutrition, detection, and social impact of diseases linked to its deficiency. Nutrients 13:1136.

Fung TC, Olson CA, Hsiao EY (2017) Interactions between the microbiota, immune and nervous systems in health and disease. Nat Neurosci 20:145-155.

Ghosh S, Pramanik S (2021) Structural diversity, functional aspects and future therapeutic applications of human gut microbiome. Arch Microbiol 203:5281-5308.

Holtzman DM, Morris JC, Goate AM (2011) Alzheimer's disease: the challenge of the second century. Sci Transl Med 3:77sr71.

Hou K, Wu ZX, Chen XY, Wang JQ, Zhang D, Xiao C, Zhu D, Koya JB, Wei L, Li J, Chen ZS (2022) Microbiota in health and diseases. Signal Transduct Target Ther 7:135.

Ichikawa Y, Yamamoto H, Hirano SI, Sato B, Takefuji Y, Satoh F (2023) The overlooked benefits of hydrogen-producing bacteria. Med Gas Res 13:108-111.

Jahnen-Dechent W, Ketteler M (2012) Magnesium basics. Clin Kidney J 5:i3-i14.
Katsuno M, Sahashi K, Iguchi Y, Hashizume A (2018) Preclinical progression of neurodegenerative diseases. Nagoya J Med Sci 80:289-298.
Kaur G, Behl T, Bungau S, Kumar A, Uddin MS, Mehta V, Zengin G, Mathew B, Shah MA, Arora S (2021) Dysregulation of the gut-brain axis, dysbiosis and influence of numerous factors on gut microbiota associated Parkinson's disease. Curr Neuropharmacol 19:233-247.
Kirkland AE, Sarlo GL, Holton KF (2018) The role of magnesium in neurological disorders. Nutrients 10:730.
Larroya A, Pantoja J, Codoñer-Franch P, Cenit MC (2021) Towards tailored gut microbiome-based and dietary interventions for promoting the development and maintenance of a healthy brain. Front Pediatr 9:705859.
Liu C, Cheng Y, Guo Y, Qian H (2021) Magnesium-L-threonate alleviate colonic inflammation and memory impairment in chronic-plus-binge alcohol feeding mice. Brain Res Bull 174:184-193.
Liu C, Yang SY, Wang L, Zhou F (2022) The gut microbiome: implications for neurogenesis and neurological diseases. Neural Regen Res 17:53-58.
Liu H, Stover KR, Sivanenthiran N, Chow J, Cheng C, Liu Y, Lim S, Wu C, Weaver DF, Eubanks JH, Song H, Zhang L (2019) Impaired spatial learning and memory in middle-aged mice with kindling-induced spontaneous recurrent seizures. Front Pharmacol 10:1077.
Ma Q, Xing C, Long W, Wang HY, Liu Q, Wang RF (2019) Impact of microbiota on central nervous system and neurological diseases: the gut-brain axis. J Neuroinflammation 16:53.
Magoč T, Salzberg SL (2011) FLASH: fast length adjustment of short reads to improve genome assemblies. Bioinformatics 27:2957-2963.
Maranduba CM, De Castro SB, de Souza GT, Rossato C, da Guia FC, Valente MA, Rettore JV, Maranduba CP, de Souza CM, do Carmo AM, Macedo GC, Silva Fde S (2015) Intestinal microbiota as modulators of the immune system and neuroimmune system: impact on the host health and homeostasis. J Immunol Res 2015:931574.
Marizzoni M, Cattaneo A, Mirabelli P, Festari C, Lopizzo N, Nicolosi V, Mombelli E, Mazzelli M, Luongo D, Naviglio D, Coppola L, Salvatore M, Frisoni GB (2020) Short-chain fatty acids and lipopolysaccharide as mediators between gut dysbiosis and amyloid pathology in Alzheimer's disease. J Alzheimers Dis 78:683-697.
Mothapo KM, Ten Oever J, Koopmans P, Stelma FF, Burm S, Bajramovic J, Verbeek MM, Rikkert MGO, Netea MG, Koopman G, van der Ven AJ (2017) Soluble TLR2 and 4 concentrations in cerebrospinal fluid in HIV/SIV-related neuropathological conditions. J Neurovirol 23:250-259.
Ojeda J, Ávila A, Vidal PM (2021) Gut microbiota interaction with the central nervous system throughout life. J Clin Med 10:1299.
Oksanen J, Simpson GL, Blanchet FG, Kindt R, Legendre P, Minchin PR, O'Hara RB, Solymos P, Stevens MHH, Szoecs E, Wagner H, Barbour M, Bedward M, Bolker B, Borcard D, Carvalho G, Chirico M, De Caceres M, Durand S, Evangelista HBA, et al. (2022) Vegan: Community Ecology Package. R package version 1.17-4. http://cran.r-project.org. Accessed October 12, 2010.
Percie du Sert N, Hurst V, Ahluwalia A, Alam S, Avey MT, Baker M, Browne WJ, Clark A, Cuthill IC, Dirnagl U, Emerson M, Garner P, Holgate ST, Howells DW, Karp NA, Lazic SE, Lidster K, MacCallum CJ, Macleod M, Pearl EJ, et al. (2020) The ARRIVE guidelines 2.0: Updated guidelines for reporting animal research. PLoS Biol 18:e3000410.
Piuri G, Zocchi M, Della Porta M, Ficara V, Manoni M, Zuccotti GV, Pinotti L, Maier JA, Cazzola R (2021) Magnesium in obesity, metabolic syndrome, and type 2 diabetes. Nutrients 13:320.
Pluta R, Januszewski S (2023) Gut microbiota neurotransmitters: influence on risk and outcome of ischemic stroke. Neural Regen Res 18:1707-1708.
Pruesse E, Quast C, Knittel K, Fuchs BM, Ludwig W, Peplies J, Glöckner FO (2007) SILVA: a comprehensive online resource for quality checked and aligned ribosomal RNA sequence data compatible with ARB. Nucleic Acids Res 35:7188-7196.
Rea IM, Gibson DS, McGilligan V, McNerlan SE, Alexander HD, Ross OA (2018) Age and age-related diseases: role of inflammation triggers and cytokines. Front Immunol 9:586.
Sahebnasagh A, Eghbali S, Saghafi F, Sureda A, Avan R (2022) Neurohormetic phytochemicals in the pathogenesis of neurodegenerative diseases. Immun Ageing 19:36.
Sato N, Morishita R (2015) The roles of lipid and glucose metabolism in modulation of β-amyloid, tau, and neurodegeneration in the pathogenesis of Alzheimer disease. Front Aging Neurosci 7:199.
Soto-Heredero G, Gómez de Las Heras MM, Gabandé-Rodríguez E, Oller J, Mittelbrunn M (2020) Glycolysis- a key player in the inflammatory response. FEBS J 287:3350-3369.
Stojanov S, Berlec A, Štrukelj B (2020) The influence of probiotics on the firmicutes/bacteroidetes ratio in the treatment of obesity and inflammatory bowel disease. Microorganisms 8:1715.
Suganya K, Koo BS (2020) Gut-brain axis: role of gut microbiota on neurological disorders and how probiotics/prebiotics beneficially modulate microbial and immune pathways to improve brain functions. Int J Mol Sci 21:7551.
Tiwari S, Atluri V, Kaushik A, Yndart A, Nair M (2019) Alzheimer's disease: pathogenesis, diagnostics, and therapeutics. Int J Nanomedicine 14:5541-5554.
Tracey TJ, Steyn FJ, Wolvetang EJ, Ngo ST (2018) Neuronal lipid metabolism: multiple pathways driving functional outcomes in health and disease. Front Mol Neurosci 11:10.
Trejo-Castro AI, Carrion-Alvarez D, Martinez-Torteya A, Rangel-Escareño C (2022) A bibliometric review on gut microbiome and Alzheimer's disease between 2012 and 2021. Front Aging Neurosci 14:804177.
Vogt NM, Kerby RL, Dill-McFarland KA, Harding SJ, Merluzzi AP, Johnson SC, Carlsson CM, Asthana S, Zetterberg H, Blennow K, Bendlin BB, Rey FE (2017) Gut microbiome alterations in Alzheimer's disease. Sci Rep 7:13537.
Wang J, Liu Y, Zhou LJ, Wu Y, Li F, Shen KF, Pang RP, Wei XH, Li YY, Liu XG (2013) Magnesium L-threonate prevents and restores memory deficits associated with neuropathic pain by inhibition of TNF-α. Pain Physician 16:E563-575.
Wang Q, Garrity GM, Tiedje JM, Cole JR (2007) Naive Bayesian classifier for rapid assignment of rRNA sequences into the new bacterial taxonomy. Appl Environ Microbiol 73:5261-5267.
Wickham H (2016) ggplot2: elegant graphics for data analysis. Springer-Verlag New York.
Wu HJ, Wu E (2012) The role of gut microbiota in immune homeostasis and autoimmunity. Gut Microbes 3:4-14.
Xiong Y, Ruan YT, Zhao J, Yang YW, Chen LP, Mai YR, Yu Q, Cao ZY, Liu FF, Liao W, Liu J (2022) Magnesium-L-threonate exhibited a neuroprotective effect against oxidative stress damage in HT22 cells and Alzheimer's disease mouse model. World J Psychiatry 12:410-424.
Zhang Q, Zhao W, Hou Y, Song X, Yu H, Tan J, Zhou Y, Zhang HT (2023) β-Glucan attenuates cognitive impairment of APP/PS1 mice via regulating intestinal flora and its metabolites. CNS Neurosci Ther 29:1690-1704.

C-Editor: Zhao M; S-Editors: Yu J, Li CH; L-Editors: Kahmeyer-Gabbe M, Yu J, Song LP; T-Editor: Jia Y